An electrochemical cell with sapphire windows for *operando* synchrotron X-ray powder diffraction and spectroscopy studies of high-power and high-voltage electrodes for metal-ion batteries

Oleg A. Drozhzhin,[a,b]* Ivan V. Tereshchenko,[a,b] Hermann Emerich,[c] Evgeny V. Antipov,[a] Artem M. Abakumov[b] and Dmitry Chernyshov[c]

[a]Chemistry Department, Lomonosov Moscow State University, Leninskie gory 1, Moscow 119991, Russian Federation, [b]Center for Electrochemical Energy Storage, Skolkovo Institute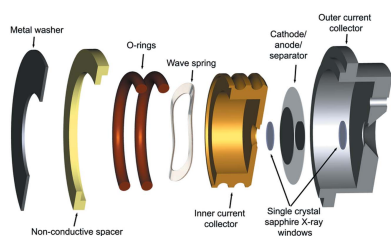 of Science and Technology, Nobel Street 3, Moscow 143026, Russian Federation, and [c]Swiss–Norwegian Beamlines, European Synchrotron, 71 Rue des Martyrs, Grenoble 38043, France. *Correspondence e-mail: drozhzhin@hotmail.com

A new multi-purpose *operando* electrochemical cell was designed, constructed and tested on the Swiss–Norwegian Beamlines BM01 and BM31 at the European Synchrotron Radiation Facility. Single-crystal sapphire X-ray windows provide a good signal-to-noise ratio, excellent electrochemical contact because of the constant pressure between the electrodes, and perfect electrochemical stability at high potentials due to the inert and non-conductive nature of sapphire. Examination of the phase transformations in the $Li_{1-x}Fe_{0.5}Mn_{0.5}PO_4$ positive electrode (cathode) material at C/2 and 10C charge and discharge rates, and a study of the valence state of the Ni cations in the $Li_{1-x}Ni_{0.5}Mn_{1.5}O_4$ cathode material for Li-ion batteries, revealed the applicability of this novel cell design to diffraction and spectroscopic investigations of high-power/high-voltage electrodes for metal-ion batteries.

1. Introduction

The application of different diffraction and spectroscopic techniques to *operando* studies of electrode materials has become an integral part of metal-ion battery research (Brant *et al.*, 2016; Harks *et al.*, 2015; Sharma *et al.*, 2015). The properties of diverse materials can be monitored *in operando*: the electrochemical mechanism (single-phase intercalation *versus* two-phase intercalation, conversion reaction, pseudo-capacity), phase transformations and stability, crystal structure transformations, the volume change between charged and discharged states, the oxidation states of the involved atomic species (*i.e. d* metals and oxygen), the local crystal and electronic structure *etc.* A vital aspect of *operando* methods stems from their inherent advantage in studying the electrochemical response of materials under non-equilibrium dynamic conditions, thus mimicking a real battery. Synchrotron radiation, in turn, provides a large choice of characterization techniques to meet these challenges: synchrotron X-ray powder diffraction (SXPD), X-ray absorption spectroscopy (XAS), X-ray fluorescence spectroscopy (XFS), X-ray photoelectron spectroscopy (XPS), small- and wide-angle scattering (SAXS and WAXS, respectively), Mössbauer spectroscopy (MS) *etc.* The first two of these methods are the most common options for metal-ion battery research as they provide relevant information on the crystal structure evolution and oxidation states of the constituent chemical species.

Various experimental setups (electrochemical cells) for *operando* SXPD and XAS studies have been developed

Metal washer — O-rings — Wave spring — Cathode/anode/separator — Outer current collector — Non-conductive spacer — Inner current collector — Single crystal sapphire X-ray windows

during the last decade (Sharma *et al.*, 2015). The principal scheme of all these cells is similar, comprising the electrochemical system consisting of a working electrode, electrolyte, counter and reference electrodes (which might be combined), current collectors, and one or several windows transparent to photons. However, some details of the cell design can play a crucial role affecting the actual functionality of the setup and the applicability of the cell to a given type of electrochemical experiment. Most of the known cell designs rely on soft polymer windows, typically Kapton films (Brant *et al.*, 2013; Kimpton & Gu, 2014; Sottmann *et al.*, 2016), which do not provide perfect electrochemical contact between the electrodes (Borkiewicz *et al.*, 2015). This can result in poor electrochemical behavior, especially at high current density, and cause irreproducibility in the obtained data. The most commonly used rigid X-ray window is a Be plate (Leriche *et al.*, 2010). However, the toxicity of beryllium and its instability at high electrode potentials (>4 V *versus* Li/Li^+) calls for alternative window materials. A possible solution to this problem has been proposed by Borkiewicz *et al.* (2012), who suggested glassy carbon Sigradur-(G) as a material for conductive rigid X-ray windows within the AMPIX cell. These windows provide uniform pressure and distribution of the electrode potential within the whole electrode stack inside the cell (Borkiewicz *et al.*, 2015). The main drawback of such a cell design is the non-negligible electrochemical activity of carbon at high (>4.8 V *versus* Li/Li^+) and low (<0.5 V *versus* Li/Li^+) potentials in contact with the metal-ion electrolyte that could give rise to instabilities while studying high-voltage cathode materials.

In this work, we address the above-mentioned challenges in *operando* X-ray powder diffraction and spectroscopy studies by constructing a universal electrochemical cell applicable to a wide range of experimental conditions, including investigations of high-power and high-voltage cathode materials for metal-ion batteries.

2. Experimental

The cell was tested on the Swiss–Norwegian Beamlines (SNBL) BM01 and BM31 at the European Synchrotron Radiation Facility (ESRF, Grenoble, France). Both tests were carried out in a low-intensity beam mode ($\sim$40 mA, 4*10 filling mode; http://www.esrf.eu/Accelerators/Operation/Modes). The PILATUS@SNBL diffractometer (Dyadkin *et al.*, 2016) was used for SXPD studies (0.7225 Å wavelength). The two-dimensional diffraction data from the Pilatus 2M detector were processed using the SNBL *Toolbox* and *BUBBLE* software (Dyadkin *et al.*, 2016). The time of data acquisition was 10 s per pattern. Sequential Rietveld refinement (*FULLPROF* program suite; Rodríguez-Carvajal, 2001) was applied to analyze the phase transformations. Ni *K*-edge X-ray absorption near-edge structure (XANES) data were collected on BM31 in transmission mode using ionization chambers in the energy range 8.3–8.4 keV and employing a double-crystal Si(111) monochromator.

The overall scheme of the present *operando* cell design is presented in Fig. 1. The cell consists of two current collectors (inner and outer). The inner collector is considered to be an anode side and can be manufactured of stainless steel or brass. The outer collector is typically a cathode side; aluminium or duralumin are the preferred materials, to prevent metal surface oxidation at high electrode potentials. One or two O-rings provide good sealing and electrical isolation between the outer and inner parts. The conical openings from both cathode and anode sides (opening angles 120° and 90°, respectively) allow X-ray detectors to be placed on both sides of the cell to enable combined SXPD/XRF or SXPD/XAS studies on BM31.

The main advantages of the cell stem from the construction and materials of the X-ray windows. We tested several materials and found that thin ($\sim$0.2 mm) sapphire single-crystal wafers provide the best combination of mechanical hardness, low background contribution to the SXPD patterns, high transparency to X-ray radiation and electrochemical stability in a high-voltage region. As sapphire is an electrical insulator, the windows cannot be used as current collectors. However, if the size of the electrodes exceeds the surface area of the windows, a good contact is formed between the electrode current collector (typically Al) and the outer cell part. In the case of small ($\varnothing < 5$ mm) electrodes, a thin Al foil has to be applied to cover the sapphire window. Bragg reflections from the sapphire single-crystal windows contribute to the X-ray diffraction pattern, but because they are well localized this contribution can be easily eliminated (masked) using the data-processing software.
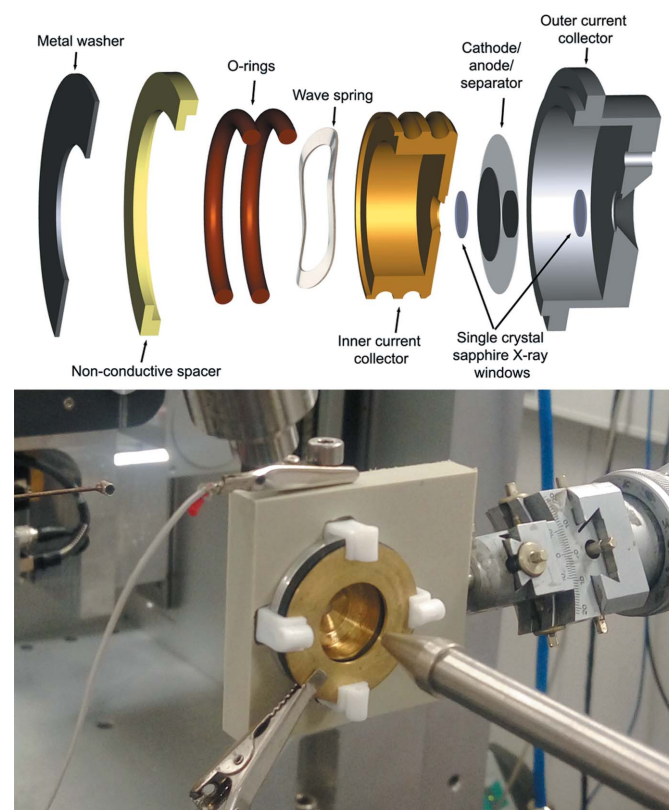

Figure 1
(Top) Exploded view and (bottom) photograph of the novel *operando* electrochemical cell.

Two types of cathode material were used to test the cell performance. A high-power $LiFe_{0.5}Mn_{0.5}PO_4$ cathode with an olivine-type structure was selected to study phase transformations at a high (10C) discharge rate. A high-voltage $LiNi_{0.5}Mn_{1.5}O_4$ material with the spinel structure was used for XANES. Electrode composites consisted of 75 mass% of the active material, 12.5 mass% of SuperC carbon and 12.5 mass% of PVDF (polyvinylidene fluoride; Solvay). Metallic Li was used as both counter and reference electrodes. A solution of 1 M $LiPF_6$ in ethylene carbonate/diethyl carbonate (EC:DEC) served as the electrolyte, impregnating a porous polypropylene membrane (Celgard) as separator.

3. Results

Phase transformations in $LiFe_{0.5}Mn_{0.5}PO_4$ were studied at a moderate charge rate (C/2) and a fast discharge rate (10C). The total time of the discharge process was 250 s, therefore 25 patterns were collected. Selected SXPD patterns on charge and discharge are presented in Fig. 2.

In spite of the very short data-acquisition time for each pattern and the low X-ray flux, the quality and resolution of the SXPD patterns are more than sufficient for further quantitative analysis with the Rietveld method. Rietveld refinement in sequential mode was employed to analyze the mass fractions of the three constituent phases and their unit-cell parameters. The results are presented in Fig. 3.

It is well known that the $LiFe_{0.5}Mn_{0.5}PO_4$ cathode material exhibits two two-phase transitions during charge and discharge (Deng *et al.*, 2017; Yamada *et al.*, 2001). First, the Li-rich $Li_{1-x}Fe_{0.5}Mn_{0.5}PO_4$ phase (denoted LFMP, $x > {\sim}0.8$) with a narrow range of x values transforms to the intermediate $Li_{1-x}Fe_{0.5}Mn_{0.5}PO_4$ phase (denoted L05FMP) with x varying between ${\sim}0.3$ and ${\sim}0.8$. After that, the intermediate phase converts into the Li-poor $Li_{1-x}Fe_{0.5}Mn_{0.5}PO_4$ phase (FMP) with $x < {\sim}0.3$. It is also known that, even at the same charge and discharge rate, a clear asymmetry between phase transformations in the Li deintercalation and insertion processes exists (Drozhzhin *et al.*, 2016; Ravnsbaek *et al.*, 2014).

Fig. 3 demonstrates that the asymmetry of the phase transformations at different charge and discharge rates is very pronounced. In fact, the triphilite-
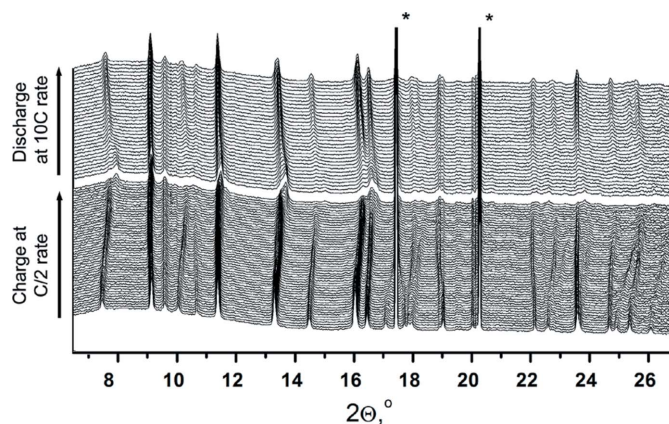

Figure 2
Selected SXPD patterns collected at charge (C/2 rate) and discharge (10C rate). The data acquisition time was 10 s per pattern. Peaks of the Al current collector are marked with asterisks.
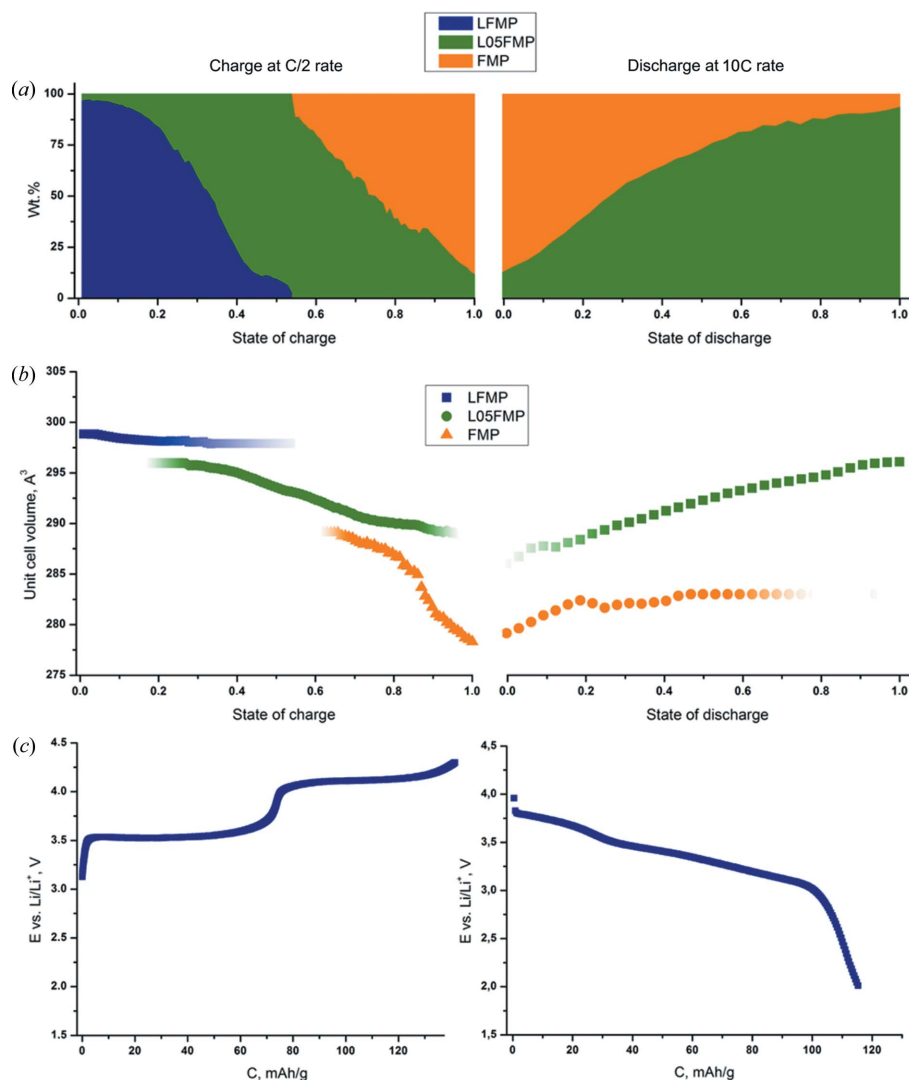

Figure 3
Results of sequential Rietveld refinement. (*a*) The mass fraction of each phase. (*b*) Their unit-cell parameters. (*c*) The corresponding *E*–*C* curves collected during charge (C/2 rate) and discharge (10C rate). The notations stand for the three distinct $Li_{1-x}Fe_{0.5}Mn_{0.5}PO_4$ phases: Li-rich (LFMP, $x > 0.8$), intermediate (L05FMP, $0.3 < x < 0.8$) and Li-poor (FMP, $x < 0.3$).

type fully lithiated phase designated as LFMP does not appear during discharge at all. Similar behavior was earlier observed for the $LiFePO_4$ cathode material (Shin *et al.*, 2008). It is assumed that, under such high discharge rates, the solid-solution behavior is preferable to the two-phase regime because of severe kinetic limitations. The lithiated phase in our experiment is formed after turning off high current or reducing its value. The obtained results correlate well with the data presented by Ravnsbaek and co-workers, who used the already mentioned AMPIX cell to study phase transformations in $LiFe_{1-x}Mn_xPO_4$ cathode materials at high current densities (Ravnsbaek *et al.*, 2016).

In a second test we aimed to investigate the possibility of XAS measurements. Besides sapphire X-ray windows, we also tested thin mica wafers, which provide a better signal-to-noise ratio for X-ray absorption spectra. We used the $LiNi_{0.5}Mn_{1.5}O_4$ spinel as a well studied high-voltage material (charge and discharge at ∼4.6–4.8 V *versus* Li/Li^+) with a two-electron transition for the Ni cations: $Ni^{2+} \leftrightarrow Ni^{3+} \leftrightarrow Ni^{4+}$. The results of the XANES measurements are presented in Fig. 4.

A pronounced shift of the absorption Ni K-edge from higher to lower energies during discharge indicates a change in the formal oxidation state of Ni from +4 to +2. The obtained data correlate well with the previously published results (Rana *et al.*, 2014; Sottmann *et al.*, 2016). Although the spectra were collected during a low-intensity beam mode (39 mA *versus* 200 mA), their quality is undoubtedly sufficient to monitor the trend. No parasitic oxidation processes were observed in the high-voltage region, either during this or any other test, reflecting the good oxidation stability of the cell components.

The results presented above, as well as the data collected for other materials, which will be published elsewhere, allow us to draw the following conclusions concerning the functionality of the cell:

(i) Rigid sapphire X-ray windows allow for sufficient and uniform pressure to be applied to the electrodes. We did not observe any significant difference in the electrochemical data obtained *in operando* and in standard laboratory two-electrode cells for the same material, even at high (≥10C) charge and discharge rates.

(ii) The electrochemical inactivity of the sapphire single crystals and usage of an Al current collector enable experiments with high-voltage cathode materials for metal-ion batteries. To study anode materials for Li-ion batteries, a stainless steel current collector (outer part) was also constructed.

(iii) A possible drawback of the presented cell design is the non-conductive nature of the X-ray windows. A thin Al foil should be used to achieve good electrical contact between the studied electrode and the Al current collector. The AMPIX cell designed by ANL (Borkiewicz *et al.*, 2012) does not have this shortcoming, but it may suffer from the electrochemical instability of carbon under certain experimental conditions.

The experiments discussed above have been performed in a single cell. However, the rather small size of the cell (31 mm in diameter) allows a number of these cells to be mounted in a single moving sample holder to obtain multiple data sets within one batch (Sottmann *et al.*, 2016).

4. Summary

A novel *operando* electrochemical cell with single-crystal sapphire X-ray windows has been designed for and successfully applied to the study of phase transformations and the valence states of the cations in high-power/high-voltage cathode materials for Li-ion batteries. The design of the cell allows simultaneous or sequential application of diffraction and spectroscopic techniques. It is particularly important to mention that this cell design allows for fluorescence detection at the outlet as well as at the inlet side of the cell. Rigid sapphire windows ensure excellent electrical contact between the electrodes and electrochemical and mechanical stability of the cell components. Currently up to 12 (BM31) and five (BM01) different materials can be studied using periodically repeating measurements with multiple cell-positioning holders constructed at SNBL. The setup is available for user experiments *via* the regular ESRF proposal scheme.

Figure 4
XANES data for the Ni K-edge collected *in operando* for the $LiNi_{0.5}Mn_{1.5}O_4$ cathode material. (*a*) Selected spectra and (*b*) the corresponding discharge E–x curve.

References

Borkiewicz, O. J., Shyam, B., Wiaderek, K. M., Kurtz, C., Chupas, P. J. & Chapman, K. W. (2012). *J. Appl. Cryst.* **45**, 1261–1269.
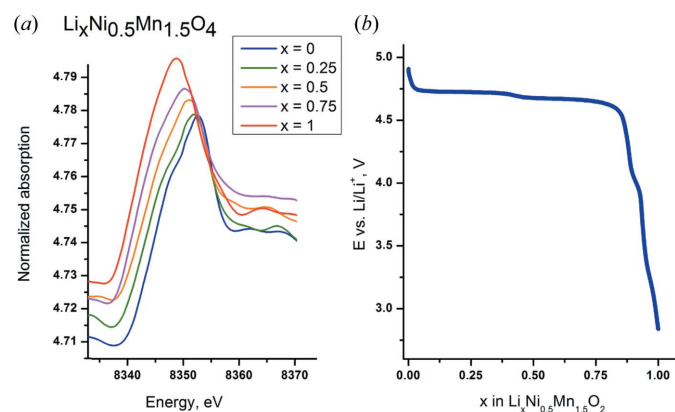
Borkiewicz, O. J., Wiaderek, K. M., Chupas, P. J. & Chapman, K. W. (2015). *J. Phys. Chem. Lett.* **6**, 2081–2085.

Brant, W. R., Li, D., Gu, Q. & Schmid, S. (2016). *J. Power Sources*, **302**, 126–134.

Brant, W. R., Schmid, S., Du, G., Gu, Q. & Sharma, N. (2013). *J. Power Sources*, **244**, 109–114.

Deng, Y., Yang, C., Zou, K., Qin, X., Zhao, Z. & Chen, G. (2017). *Adv. Energ. Mater.* **7**, 1601958.

Drozhzhin, O. A., Sumanov, V. D., Karakulina, O. M., Abakumov, A. M., Hadermann, J., Baranov, A. N., Stevenson, K. J. & Antipov, E. V. (2016). *Electrochim. Acta*, **191**, 149–157.

Dyadkin, V., Pattison, P., Dmitriev, V. & Chernyshov, D. (2016). *J. Synchrotron Rad.* **23**, 825–829.

Harks, P. P. R. M. L., Mulder, F. M. & Notten, P. H. L. (2015). *J. Power Sources*, **288**, 92–105.

Kimpton, J. & Gu, Q. (2014). *Synchrotron Rad. News*, **27**, 18–20.

Leriche, J. B., Hamelet, S., Shu, J., Morcrette, M., Masquelier, C., Ouvrard, G., Zerrouki, M., Soudan, P., Belin, S., Elkaïm, E. & Baudelet, F. (2010). *J. Electrochem. Soc.* **157**, A606–A610.

Rana, J., Glatthaar, S., Gesswein, H., Sharma, N., Binder, J. R., Chernikov, R., Schumacher, G. & Banhart, J. (2014). *J. Power Sources*, **255**, 439–449.

Ravnsbaek, D. B., Xiang, K., Xing, W., Borkiewicz, O. J., Wiaderek, K. M., Gionet, P., Chapman, K. W., Chupas, P. J. & Chiang, Y. M. (2014). *Nano Lett.* **14**, 1484–1491.

Ravnsbaek, D. B., Xiang, K., Xing, W., Borkiewicz, O. J., Wiaderek, K. M., Gionet, P., Chapman, K. W., Chupas, P. J., Tang, M. & Chiang, Y. M. (2016). *Nano Lett.* **16**, 2375–2380.

Rodríguez-Carvajal, J. (2001). *IUCr Commission Powder Diffr. Newsl.* **26**, 12–19.

Sharma, N., Pang, W. K., Guo, Z. & Peterson, V. K. (2015). *ChemSusChem*, **8**, 2826–2853.

Shin, H. C., Chung, K. Y., Min, W. S., Byun, D. J., Jang, H. & Cho, B. W. (2008). *Electrochem. Commun.* **10**, 536–540.

Sottmann, J., Homs-Regojo, R., Wragg, D. S., Fjellvåg, H., Margadonna, S. & Emerich, H. (2016). *J. Appl. Cryst.* **49**, 1972–1981.

Yamada, A., Kudo, Y. & Liu, K.-Y. (2001). *J. Electrochem. Soc.* **148**, A1153–A1158.